

Structural evolution in iron tellurates

A. van der Lee^{a,*}, R. Astier^{b,1}

^aInstitut Européen des Membranes, UMR 5635, cc 047 Université de Montpellier II, 34095 Montpellier, France

^bLaboratoire de Chimie Moléculaire et Organisation du Solide, UMR 5253, cc 007 Université de Montpellier II, 34095 Montpellier, France

Received 20 November 2006; received in revised form 10 January 2007; accepted 12 January 2007

Available online 2 February 2007

Abstract

Three new members within the iron tellurate family have been synthesized and characterized by single-crystal diffraction. $\text{Fe}_2\text{Te}_3\text{O}_9$ is orthorhombic, $a = 7.80240(10)\text{Å}$, $b = 17.7501(3)\text{Å}$, $c = 5.28050(10)\text{Å}$, $Z = 4$, space group $Pnma$, final agreement factors $R_1 = 0.0261$ ($wR_2 = 0.0688$) for 1271 independent reflections. $\text{Fe}_3\text{Te}_4\text{O}_{12}$ is monoclinic, $a = 9.1312(2)\text{Å}$, $b = 7.3554(2)\text{Å}$, $c = 15.7379(3)\text{Å}$, $\beta = 107.950(10)^\circ$, $Z = 4$, space group $P2_1/c$, final agreement factors $R_1 = 0.0380$ ($wR_2 = 0.0281$) for 3302 independent reflections. $\text{FeTe}_6\text{O}_{13}$ is trigonal, $a = b = 10.16630(10)\text{Å}$, $c = 18.9330(3)\text{Å}$, $Z = 6$, space group $R\bar{3}m$, final agreement factors $R_1 = 0.0309$ ($wR_2 = 0.0641$) for 1264 independent reflections. Together with the four already known members of the family, Fe_2TeO_5 , Fe_2TeO_6 , and $\text{Fe}_2\text{Te}_3\text{O}_9$ (a dimorphic variant of the afore-mentioned structure with the same chemical formula), and $\text{Fe}_2\text{Te}_4\text{O}_{11}$, the iron tellurates now span from relatively Fe-rich and Te-poor to relatively Fe-poor to Te-rich compounds. The structural diversity within Fe–Te–O system is discussed in terms of the lone-pair stereochemistry of the Te^{4+} anion and the cross-over from Fe^{3+} to mixed-valence $\text{Fe}^{3+}/\text{Fe}^{2+}$ and Fe^{2+} coordination polyhedra compounds.

© 2007 Elsevier Inc. All rights reserved.

PACS: 61.10.Nz; 61.66.–f; 61.66.Fn

Keywords: Iron tellurates; Electronic lone pairs; Tunnel structure; Ab initio structure determination

1. Introduction

The crystal chemistry of tellurates is dominated by the possibility having either an oxidation state 4+ or 6+ for tellurium. In a number of cases the two oxidation states co-exist in the same structure, e.g. in Te_2O_5 [1], Te_4O_9 [2], $\text{K}_2\text{Te}_4\text{O}_{12}$ [3], BaTe_2O_6 [4], and SrTe_3O_8 [5]. Whereas Te(VI) exhibits octahedral coordination, the Te(IV) coordination is much more varied thanks to the stereoactivity of its lone pair. In the seventies of the last century the structures of four different iron tellurates, Fe_2TeO_5 [6,7], Fe_2TeO_6 [8], $\text{Fe}_2\text{Te}_4\text{O}_{11}$ [9], and $\text{Fe}_2\text{Te}_3\text{O}_9$ [10] were determined, which showed already the richness of the crystal chemistry within this family of compounds. To

complete the study we determined the structures of three new compounds which show a cross-over from Fe^{3+} to Fe^{2+} compounds, including a mixed-valent $\text{Fe}^{2+}/\text{Fe}^{3+}$ compound.

2. Experimental section

2.1. Syntheses

The three compounds were obtained by hydrothermal synthesis using commercially available chemicals (1 μm -sized Fe_3O_4 , Fe_2O_3 , and TeO_2 powders) used as received, in a reactor with a free volume V_{int} of 56 ml, closed by copper Bridgmann seals. The molar Fe_3O_4 to TeO_2 ratio for the compound with final composition $\text{Fe}_3\text{Te}_4\text{O}_{12}$ was 1 : 1, for $\text{FeTe}_6\text{O}_{13}$ 2 : 9 and the molar Fe_2O_3 to TeO_2 ratio for $\text{Fe}_2\text{Te}_3\text{O}_9$ was 1 : 3. The mixtures were introduced in gold tubes to which several water drops acidified with some HCl to a pH of 4–5 were added before arc sealing. The sealing was tested by weighting the tubes before and after

*Corresponding author. Fax: +33 4 67 14 91 19.

E-mail address: avderlee@univ-montp2.fr (A. van der Lee).

¹Present address: Institut de Chimie Séparative de Marcoule, UMR 5257, CEA/VRH/ICSM Centre de Marcoule, BP 17171, 30207 Bagnols sur Cèze, France.

one night under vacuum conditions. The tubes were also weighted before filling as to know the volume of the constituents in each tube. From the volume V_{Cl} of the constituents and the free volume V_{int} the quantity of water to be introduced in the reactor can be calculated by $(V_{\text{int}} - V_{\text{Cl}}) * CR$ where CR is the filling coefficient determined according to the PVT curves of Kennedy [11] for water, $CR = 63.9\%$. The pressure was approximately 2000 bar and the temperature 560 °C. The bomb was left in the furnace for 48 h at this temperature and then cooled to room temperature. The resulting products, consisting of brown-red plate or block single crystals, were filtered, washed with distilled water and dried under ambient conditions.

2.2. X-ray single-crystal diffraction

The single-crystal data were collected at 173 K using an Xcalibur-I four-circle diffractometer (Oxford-Diffraction) with graphite monochromatized Mo-K α radiation. ω -scans were used in all cases; typical data collection times were 17–22 h. The intensities were extracted from the recorded images by the “Proffit” algorithm such as implemented in the RED program [12]. Further details about the data collection are given in Table 1. The intensities were corrected for Lorentz-polarization effects and absorption and scale variation corrections were applied using the AbsPack algorithm of the RED program [12]. The space group $P2_1/c$ for compound $\text{Fe}_3\text{Te}_4\text{O}_{12}$ was determined unambiguously from the systematic reflection conditions, whereas for the data set of compound $\text{Fe}_2\text{Te}_3\text{O}_9$ the centrosymmetric group prevailed for the choice $Pnma$

versus $Pn2_1a$. For the reflection data set of compound $\text{FeTe}_6\text{O}_{13}$ with extinction symbol R —the choice fall on the three candidate space groups in Laue class $\bar{3}m$ because of an approximately equal internal R -factor R_{int} for the Laue classes $\bar{3}$ and $\bar{3}m$. Out of the three possible groups the centrosymmetric space group $R\bar{3}m$ was selected, which proved to be correct during the refinement. All three structures were *ab initio* solved using the charge-flipping algorithm [13] such as implemented in the BayMEM program [14]; default values for the flipping parameters were used. Note that *a priori* space group information is not used in the charge-flipping algorithm. The correct space group can be inferred from the resulting electron density map and thus independently checked with the choice from the reflection conditions. Another feature of the charge-flipping algorithm is that *a priori* knowledge about the composition is not required, this in contrast with conventional direct methods, where at least approximate knowledge about the composition has to be provided. The CRYSTALS program suite [15] was used to refine the structures. All independent reflections were used for non-linear least-squares refinement on $|F|^2$. A parameter describing secondary extinction was added to each refinement. All atoms were refined anisotropically. Selected refinement details, including cell parameters, are given in Table 1. Atomic coordinates and equivalent isotropic displacement parameters are listed in Table 2. Selected distances for the three compounds are compiled in Tables 3–5. Further details of the crystal structure investigation may be obtained from the Fachinformationszentrum Karlsruhe, 76344 Eggenstein-Leopoldshafen, Germany (fax: (+49) 7247-808-666; e-mail: crysdata@fiz-karlsruhe.de) on quoting the depository number

Table 1
Crystal data for $\text{Fe}_3\text{Te}_4\text{O}_{12}$, $\text{Fe}_2\text{Te}_3\text{O}_9$, $\text{FeTe}_6\text{O}_{13}$

	$\text{Fe}_3\text{Te}_4\text{O}_{12}$	$\text{Fe}_2\text{Te}_3\text{O}_9$	$\text{FeTe}_6\text{O}_{13}$
Crystal color, habit	Red-brown, plate	Red-brown, prism	Red-brown, plate
Crystal size	$0.30 \times 0.06 \times 0.16$	$0.06 \times 0.30 \times 0.33$	$0.03 \times 0.23 \times 0.23$
Crystal system, space group	Monoclinic, $P2_1/c$	Orthorhombic, $Pnma$	Trigonal, $R\bar{3}m$
a	9.1312(2) Å	7.80240(10) Å	10.16630(10) Å
b	7.3554(2) Å	17.7501(3) Å	10.16630(10) Å
c	15.7379(3) Å	5.28050(10) Å	18.9330(3) Å
α	90°	90°	90°
β	107.95(1)°	90°	90°
γ	90°	90°	120°
Volume	1005.57(7) Å ³	731.31(2) Å ³	1694.63(4) Å ³
Z , Calculated density	4, 5.75 g cm ⁻³	4, 5.80 g cm ⁻³	6, 6.052 g cm ⁻³
Formula weight	869.93	638.49	1029.45
Reflections recorded/unique/used ^a	17235/3308/3302	11862/1272/1271	9461/1268/1264
R_{int}	0.033	0.055	0.035
No reflections with $I \geq 2\sigma(I)$	1963	1186	1115
No. variables	173	68	62
Residual electron densities (eÅ ⁻³)	-2.4, 2.4	-1.8, 2.2	-3.2, 3.5
Goodness of fit	0.527	1.018	1.029
Final R indices (all data)	0.0380, 0.0281	0.0261, 0.0688	0.0309, 0.0641

^aUnique reflections are those reflections that remain after averaging recorded reflections according to the Laue class; used reflections are those reflections from the set of unique reflections that were used for the least-squares refinement. Reflections with $(\sin \theta/\lambda)^2 \leq 0.01$ were rejected, because they are close to the beamstop and possibly partially obscured.

Table 2

Atomic coordinates and equivalent isotropic displacement parameters for $\text{Fe}_3\text{Te}_4\text{O}_{12}$, $\text{Fe}_2\text{Te}_3\text{O}_9$, and $\text{FeTe}_6\text{O}_{13}$

Atom	x	y	z	U _{eq}
<i>Fe₃Te₄O₁₂</i>				
Fe(1)	0.32385(7)	0.36752(11)	0.19769(4)	0.0074
Fe(2)	0.57436(7)	0.11834(12)	0.09727(4)	0.0084
Fe(3)	0.68518(7)	0.36995(10)	0.30664(4)	0.0065
Te(4)	0.44973(3)	0.11898(5)	0.365440(17)	0.0079
Te(5)	0.17756(3)	0.12817(5)	−0.010316(17)	0.0062
Te(6)	0.16339(3)	−0.13947(5)	0.468896(17)	0.0076
Te(7)	−0.01456(3)	0.11158(5)	0.252904(19)	0.0059
O(8)	0.1957(4)	0.3183(4)	0.0734(2)	0.0110
O(9)	0.3244(3)	0.1179(5)	0.23768(16)	0.0067
O(10)	0.4733(3)	0.3974(5)	0.32998(17)	0.0068
O(11)	0.6401(3)	0.1176(4)	0.33674(16)	0.0063
O(12)	0.3807(3)	0.1115(5)	−0.01157(19)	0.0122
O(13)	0.4630(3)	−0.1607(4)	0.32860(19)	0.0078
O(14)	0.1899(4)	−0.0699(4)	0.0677(2)	0.0084
O(15)	0.3743(3)	−0.1308(6)	0.49459(19)	0.0182
O(16)	0.1218(4)	0.0560(4)	0.3839(2)	0.0134
O(17)	−0.1536(3)	−0.0738(4)	0.2538(2)	0.0118
O(18)	−0.1199(3)	0.3011(4)	0.28765(19)	0.0077
O(19)	0.8320(4)	0.1675(5)	0.1124(2)	0.0199
<i>Fe₂Te₃O₉</i>				
Fe(1)	−0.20196(7)	−0.06442(3)	0.70772(9)	0.0039
Te(2)	−0.38274(3)	−0.126153(12)	0.18630(4)	0.0036
Te(3)	−0.15929(4)	3/4	0.77774(6)	0.0037
O(4)	−0.4543(3)	−0.07063(14)	0.8876(5)	0.0056
O(5)	−0.2214(3)	−0.17096(15)	0.5495(5)	0.0063
O(6)	−0.3166(3)	−0.03590(14)	0.3781(5)	0.0056
O(7)	−0.3704(5)	3/4	0.9592(8)	0.0074
O(8)	−0.1635(3)	−0.12246(14)	0.0259(5)	0.0054
<i>FeTe₆O₁₃</i>				
Fe(1)	2/3	1/3	0.07698(6)	0.0034
Te(2)	0.10095(3)	0.49485(4)	0.076291(15)	0.0049
Te(3)	0.74869(4)	0.56989(4)	0.238320(17)	0.0092
O(4)	2/3	1/3	0.2485(3)	0.0088
O(5)	0.7782(4)	0.5355(4)	0.14061(18)	0.0083
O(6)	0.2787(4)	0.4831(4)	0.0977(2)	0.0075
O(7)	0.0017(4)	0.2529(4)	0.0518(2)	0.0096
O(8)	0.1395(4)	0.5254(4)	−0.02013(18)	0.0075

CSD-417291, CSD-417292, and CSD-417293 for $\text{Fe}_2\text{O}_9\text{Te}_3$, $\text{Fe}_3\text{O}_{12}\text{Te}_4$, and $\text{FeO}_{13}\text{Te}_6$, respectively. The structural drawings were made using DRAWxtl [16].

3. Discussion

In order to generalize the discussion to all known members of the iron tellurate family, first the results of the bond valence calculations are discussed. Table 6 lists the bond valence sums (BVSs) calculated using VaList [17] and bond valence parameters from Brown and Altermatt [18], together with the iron and tellurium to oxygen ratios. The BVS values yield for each compound, taking into account the site multiplicities for each individual atom, overall charge neutrality. The calculations show that hexavalent Te only exists in the Te-poorest compound, whereas bivalent Fe starts to dominate for the compounds that

Table 3

Bond distances (Å) in the structure of $\text{Fe}_3\text{Te}_4\text{O}_{12}$

Fe1–O13 ^a	2.121(3)	Fe3–O14 ^d	2.004(3)	Te5–O12	1.865(3)
Fe1–O17 ^b	1.979(3)	Fe3–O18 ^c	1.960(3)	Te5–O14	1.887(3)
Fe1–O11 ^a	1.974(3)	Fe3–O9 ^a	1.945(3)	Te6–O14 ^d	2.611(3)
Fe1–O8	1.978(3)	Fe3–O10	2.087(3)	Te6–O19 ^e	1.920(3)
Fe1–O9	1.940(3)	Fe3–O11	1.990(3)	Te6–O15	1.843(3)
Fe1–O10	2.120(3)	Te4–O15 ^f	2.294(3)	Te6–O16	1.920(3)
Fe2–O12 ^g	2.278(4)	Te4–O9	1.984(2)	Te7–O19 ^j	2.261(3)
Fe2–O10 ^e	2.109(3)	Te4–O10	2.151(3)	Te7–O18 ^h	2.759(3)
Fe2–O13 ^a	2.089(3)	Te4–O11	1.926(2)	Te7–O17 ^b	2.797(3)
Fe2–O15 ^a	2.476(4)	Te4–O13	2.151(3)	Te7–O16	2.094(3)
Fe2–O12	2.048(3)	Te5–O19 ^g	2.689(3)	Te7–O17	1.866(3)
Fe2–O19	2.319(4)	Te5–O16 ⁱ	2.811(3)	Te7–O18	1.869(3)
Fe3–O13 ^a	2.153(3)	Te5–O8	1.894(3)		

Note: Symmetry operations used to generate equivalent atoms.

$$^a 1 - x, \frac{1}{2} + y, \frac{1}{2} - z.$$

$$^b -x, \frac{1}{2} + y, \frac{1}{2} - z.$$

$$^c 1 + x, y, z.$$

$$^d x, -\frac{1}{2} - y, \frac{1}{2} + z.$$

$$^e 1 - x, -\frac{1}{2} + y, \frac{1}{2} - z.$$

$$^f 1 - x, -y, 1 - z.$$

$$^g 1 - x, -y, -z.$$

$$^h -x, -\frac{1}{2} + y, \frac{1}{2} - z.$$

$$^i x, \frac{1}{2} - y, -\frac{1}{2} + z.$$

$$^j -1 + x, y, z.$$

Table 4

Bond distances (Å) in the structure of $\text{Fe}_2\text{Te}_3\text{O}_9$

Fe1–O6 ^a	2.000(3)	Te2–O7 ^b	2.506(2)	Te3–O7 ^c	2.578(4)
Fe1–O4 ^d	2.000(3)	Te2–O8 ^e	2.667(3)	Te3–O8 ^f	2.616(3)
Fe1–O8 ^f	1.993(3)	Te2–O4 ^g	1.942(2)	Te3–O8 ^h	2.616(3)
Fe1–O4	2.189(3)	Te2–O5	2.428(3)	Te3–O5 ⁱ	1.912(3)
Fe1–O5	2.073(3)	Te2–O6	1.964(3)	Te3–O5	1.912(3)
Fe1–O6	2.021(3)	Te2–O8	1.910(3)	Te3–O7	1.905(4)

Note: Symmetry operations used to generate equivalent atoms.

$$^a \frac{3}{2} - x, 2 - y, \frac{1}{2} + z.$$

$$^b x, \frac{3}{2} - y, -1 + z.$$

$$^c \frac{1}{2} + x, \frac{3}{2} - y, \frac{3}{2} - z.$$

$$^d \frac{1}{2} + x, -y, \frac{3}{2} - z.$$

$$^e -\frac{1}{2} + x, y, \frac{1}{2} - z.$$

$$^f x, y, 1 + z.$$

$$^g x, y, -1 + z.$$

$$^h x, \frac{3}{2} - y, z.$$

$$^i x, \frac{3}{2} - y, z.$$

are poorest in Fe. The iron coordination is always six, but the octahedra are more regular for trivalent Fe than for bivalent Fe. The structural distribution of the Fe octahedra is shown in Fig. 1. The Fe octahedra tend to arrange themselves in layers, the only structure being really three-dimensional with respect to the distribution of the Fe-octahedra, is Fe_2TeO_6 , which is not amazing, because it is the only structure within the series that has only hexavalent Te ions, which themselves are coordinated octahedrally by oxygen. The electronic lone pairs present in the other six structures have apparently a very structure directing effect. Face-sharing of Fe octahedra only occurs once in this series; edge-sharing is evidently the predominant linking

Table 5
Bond distances (Å) in the structure of FeTe₆O₁₃

Fe1–O5 ^a	2.152(4)	Fe1–O5	2.152(4)	Te2–O8	1.860(3)
Fe1–O5 ^b	2.152(4)	Te2–O8 ^c	2.578(4)	Te3–O5 ^d	2.200(4)
Fe1–O8 ^e	2.067(4)	Te2–O6 ^f	2.037(3)	Te3–O7 ^e	1.858(4)
Fe1–O8 ^h	2.067(4)	Te2–O6	1.913(3)	Te3–O4	2.1238(7)
Fe1–O8 ⁱ	2.067(4)	Te2–O7	2.191(4)	Te3–O5	1.934(3)

Note: Symmetry operations used to generate equivalent atoms.

^a $1 - y, x - y, z$.

^b $1 + x - y, 1 - x, z$.

^c $-x, 1 - y, z$.

^d $\frac{5}{3} - x, \frac{4}{3} - y, \frac{1}{3} - z$.

^e $y, -x + y, -z$.

^f $-x + y, 1 - x, z$.

^g $\frac{2}{3} + y, \frac{1}{3} - x + y, \frac{1}{3} - z$.

^h $1 - x + y, x, -z$.

ⁱ $1 - x, 1 - y, z$.

Table 6
Bond valence sums (BVSs), Fe:O and Te:O ratios and mean atomic volumes (in Å³)

Compound	Atom	BVS	Assumed	Fe:O ratio	Te:O ratio	Atomic volume
Fe ₂ TeO ₅ ^a	Fe(1)	2.942	3	1:2.5	1:5	12.45
	Fe(2)	3.048	3			
	Te(1)	3.694	4			
Fe ₂ TeO ₆ ^b	Fe(1)	3.178	3	1:3	1:6	10.68
	Te(1)	5.490	6			
Fe ₃ Te ₄ O ₁₂ ^c	Fe(1)	3.030	3	1:4	1:3	13.23
	Fe(2)	1.745	2			
	Fe(3)	2.995	3			
	Te(1)	3.804	4			
	Te(2)	4.131	4			
	Te(3)	3.950	4			
	Te(4)	4.112	4			
Fe ₂ Te ₃ O ₉ ^d	Fe(1)	2.740	3	1:4.5	1:3	13.05
	Te(1)	4.541	4			
	Te(2)	4.017	4			
Fe ₂ Te ₃ O ₉ ^e	Fe(1)	2.807	3	1:4.5	1:3	14.01
	Te(1)	4.152	4			
	Te(2)	4.024	4			
Fe ₂ Te ₄ O ₁₁ ^f	Fe(1)	3.023	3	1:5.5	1:2.9	14.08
	Fe(2)	2.888	3			
	Te(1)	4.054	4			
	Te(2)	3.870	4			
	Te(2)	4.206	4			
FeTe ₆ O ₁₃ ^g	Fe(1)	2.19	2	1:13	1:2.2	14.11
	Te(1)	4.169	4			
	Te(2)	3.721	4			

^a Astier [6] and Jumas et al. [7].

^b Kunnmann et al. [8].

^c This work.

^d This work.

^e Astier et al. [10].

^f Pertlik et al. [9].

^g This work.

for the structures with the highest Fe:O ratio. Structures with low Fe:O ratios show a transition from isolated corner-shared octahedron dimers to completely isolated Fe–O₆ octahedra.

Interesting is how for the dimorphic structures of Fe₂Te₃O₉ the same structural formula leads to a different distribution and linking of FeO₆ octahedra. Both structures are layer-like with respect to their Fe–O₆ octahedron distribution, but whereas in Fe₂Te₃O₉ (d) only face-sharing Fe₂O₉ bi-octahedra are found, in Fe₂Te₃O₉ (e) all octahedra within the quasidouble-layer are linked by corner-sharing. It is noted that the two structures have been obtained under quite different conditions. The compound in Fig. 1(d) was synthesized at atmospheric pressure under arc heating at 650 °C in an Ar flux followed by slow cooling [6], whereas the dimorphic variant in Fig. 1(e) was obtained under hydrothermal conditions at $P = 2000$ bar and 560 °C (see Section 2.1). A fast comparison between the lattice energies of the two variants can be done using the formalism developed by Glasser and Jenkins [19] which uses only cell volumes, formal charges and a modified and generalized Kapustinskii equation, and which appears to be remarkably accurate compared to direct energy calculational procedures provided the potential energy is lower than -5000 kJ mol⁻¹. In the case of dimorphic variants with the same space group, *Pnma*, and the same charge distribution, Table 6, Glasser and Jenkin's equation reduces to a comparison of the cube roots of the cell volumes. Taking the cell volumes $V = 784.7$ and 731.3 Å³ for the compound determined earlier [6,7] and the one determined in this paper, respectively, potential energies of -4978 and -5100 kJ mol⁻¹ are found, which is just on the borderline for which the method is assumed to be valid. In view of the synthesis methods for both compounds, this is in contradiction with what is expected. It is noted that a correction should be applied to the cell volumes because the earlier determined structure was done at room temperature whereas the newly determined one was determined at 175 K, but this correction cannot compensate for the rather large difference between the energies. A more detailed energy calculation is needed, possibly taking into account the special role of the lone pairs in order to explain the formation of the compounds, but this is beyond the scope of this paper.

A special note deserves the presence of one Fe²⁺ and 2Fe³⁺ ions in the structure of Fe₃Te₄O₁₂. Table 3 shows that the Fe²⁺ octahedral coordination is much more distorted than those of Fe³⁺, with Fe–O distances ranging from 2.048 to 2.476 Å for Fe²⁺, and 1.940 to 2.121 Å and 1.960 to 2.153 Å for the two Fe³⁺ ions, respectively. The structure contains one Fe₂²⁺O₁₀ bi-octahedron—internally edge-sharing—that is cornerlinked to two Fe₂³⁺O₁₀ bi-octahedron which themselves are mutually corner-linked. Fig. 2 shows the linking of two pairs of Fe³⁺ octahedra and one pair of Fe²⁺ octahedra, as well as the structural distortions for the two types of octahedra.

It is known that tellurate structures containing tetra-valent Te could contain TeO₃ trigonal pyramids, TeO₃₊₁ polyhedra with three short distances ranging from 1.86 to 1.95 Å, or TeO₄ disphenoids, each having a well defined 5s² lone pair. Higher-order TeO_{*n*} polyhedra are equally well

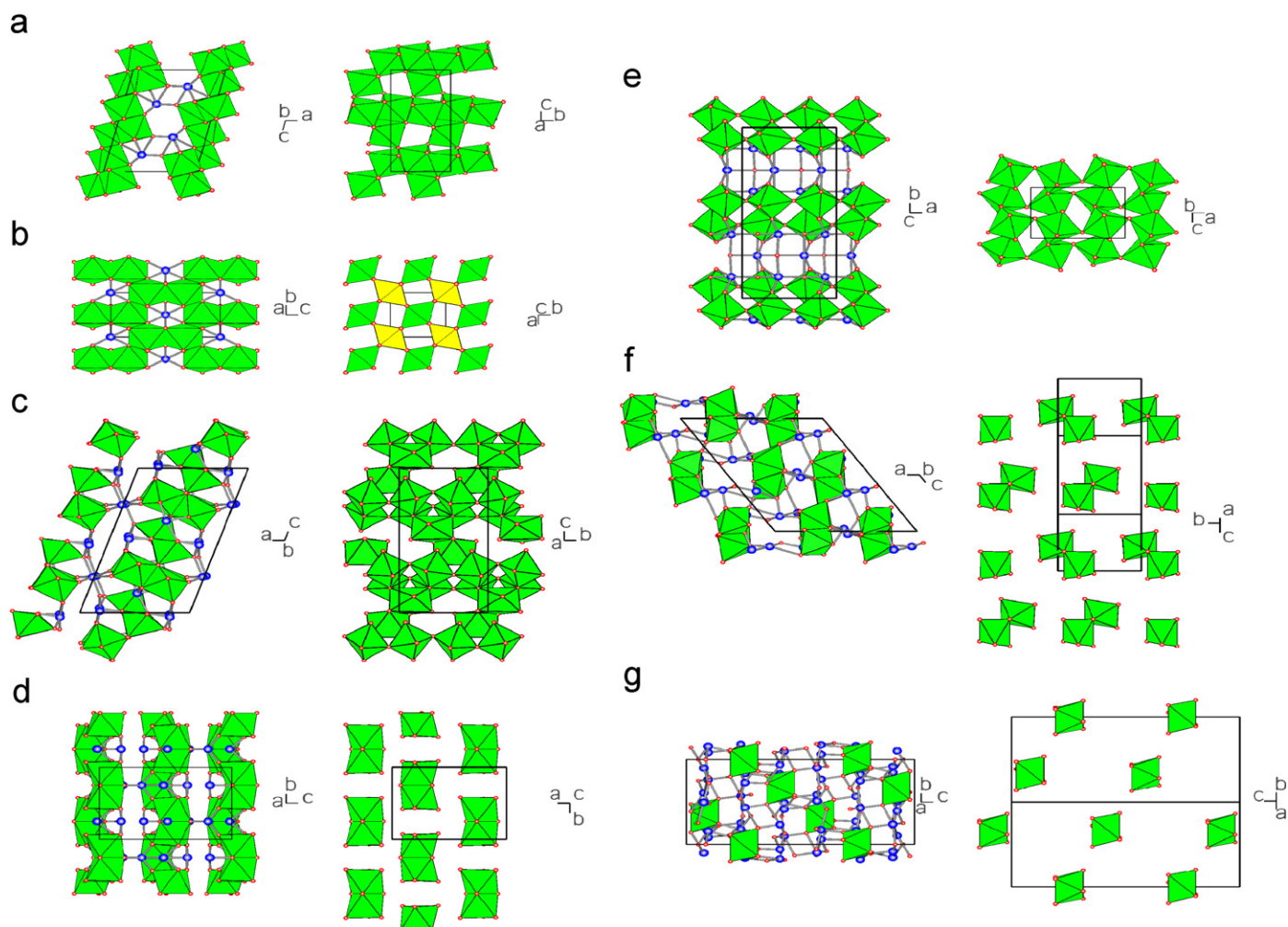


Fig. 1. FeO_6 octahedra in iron tellurates. (a) Fe_2TeO_5 , (b) Fe_2TeO_6 , (c) $\text{Fe}_3\text{Te}_4\text{O}_{12}$, (d) $\text{Fe}_2\text{Te}_3\text{O}_9$, (e) $\text{Fe}_2\text{Te}_3\text{O}_9$, (f) $\text{Fe}_2\text{Te}_4\text{O}_{11}$, (g) $\text{FeTe}_6\text{O}_{13}$. The left figure for each structure shows the arrangements of the (bi)layers of FeO_6 octahedra, whereas the right figure shows a top view of an individual (bi)layer. Fe cations are not visible, because they are in the center of an octahedron, the oxygens are indicated as small spheres and Te anions as larger spheres. Only bonds between Te and O are indicated.

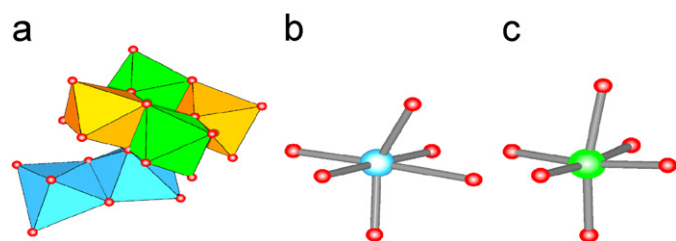


Fig. 2. Detailed view of the linking of Fe^{2+} and Fe^{3+} octahedra in the structure of $\text{Fe}_3\text{Te}_4\text{O}_{12}$ (a); structural distortions in a Fe^{2+} octahedron (b) and a Fe^{3+} octahedron (c). In (a) the two lower strongly distorted octahedra correspond to Fe^{2+} octahedra, whereas the four upper more regular octahedra correspond to two times two crystallographic independent Fe^{3+} octahedra.

found with $n = 5, 6$, but with the fifth and/or sixth Te–O distance at values larger than 2.7 \AA , lower than the sum of the Van der Waals radii for Te and O (3.58 \AA), but contributing only little—in the order of 0.1–0.2—to the BVS in the hypothesis of tetravalent Te. The presence of

the electron lone pair has on the one hand a segregating effect—the Fe-octahedra appear to arrange themselves in (bi)layers (see Fig. 1)—and on the other hand to create a non-negligible amount of empty space in the structure. It is indeed known that the Te lone pair occupies a volume that is comparable to that of an O-ion [20]. For the present family this is illustrated by the volume per atom calculated from the composition and the cell volume (see Table 6). The structure with hexavalent Te and thus without lone pairs has clearly the densest structure with 10.68 \AA^3 per atom. Structures that are relatively rich in Te have a higher concentration of lone pairs and thus a relatively high—apparent—occupied volume per atom. The empty space that is occupied by the lone pairs has the tendency to elongate itself in tunnel-like structures. The position of the lone pairs was calculated using the method developed by Galy et al. [20] and extended by Savariault [21] and found to be in very good agreement with a simpler algorithm used in the drawing program DRAWxtl [16,22]. The distance between the Te^{IV} anion and the lone pair turns out to be in

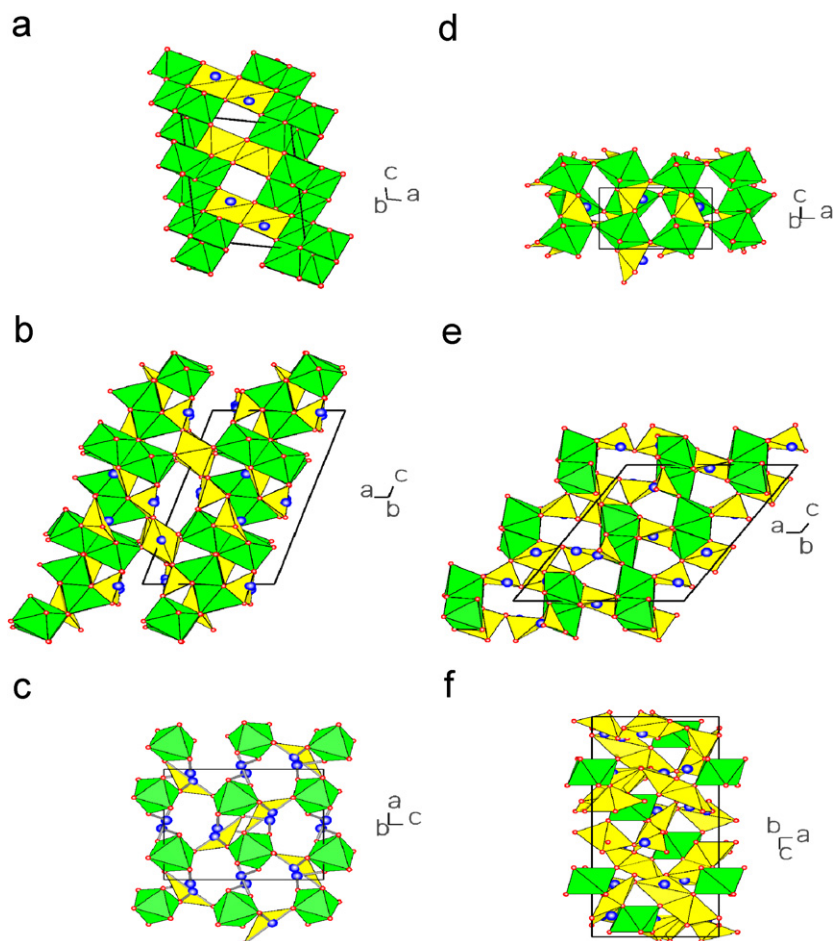


Fig. 3. $\text{Te}^{\text{IV}}\text{O}_n$ polyhedra in iron tellurates. (a) Fe_2TeO_5 , (b) $\text{Fe}_3\text{Te}_4\text{O}_{12}$, (c) $\text{Fe}_2\text{Te}_3\text{O}_9$, (d) $\text{Fe}_2\text{Te}_3\text{O}_9$, (e) $\text{Fe}_2\text{Te}_4\text{O}_{11}$, (f) $\text{FeTe}_6\text{O}_{13}$.

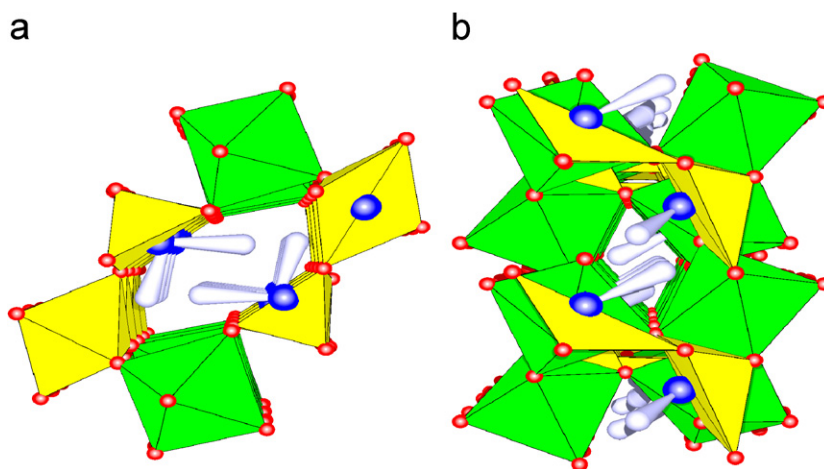


Fig. 4. Perspective views of the lone-pair tunnels in the structures of (a) $\text{Fe}_3\text{Te}_4\text{O}_{12}$ and (b) $\text{Fe}_2\text{Te}_3\text{O}_9$.

all cases approximately 1.25 Å. Fig. 3 shows effectively that in all structures except in that of the Te-richest, viz. $\text{FeTe}_6\text{O}_{13}$, tunnels are present which are more or less obstructed by the Te^{IV} -lone pairs. The two tunnel structures that were newly determined in this study, viz. those of $\text{Fe}_3\text{Te}_4\text{O}_{12}$ and $\text{Fe}_2\text{Te}_3\text{O}_9$, respectively, are shown in perspective view in Fig. 4. The lone pair cones are not

directed to the center of the tunnel, but in the direction of a corner-linking oxygen between a Te and a FeO_6 octahedron on the other side of the tunnel in the case of $\text{Fe}_3\text{Te}_4\text{O}_{12}$, whereas in the case of $\text{Fe}_2\text{Te}_3\text{O}_9$ three cones are approximately directed to three off-center sides in rather large voids that are regularly spaced along the tunnel direction. Examples of other tellurite structures having

similar tunnels obstructed by Te^{IV} -lone pairs were reported by Oufkir et al., $\text{PbTe}_5\text{O}_{11}$ [23], and more recently by Barrier et al., SrTe_3O_8 [24], and Chagraoui et al., $\text{Bi}_2\text{Te}_5\text{WO}_{16}$ [25]. With respect to the three newly determined structures in this paper only one appears to be isotopic with an already known structure, viz. the structure of $\text{Fe}_2\text{Te}_3\text{O}_9$ is isotopic with that of $\text{In}_2\text{Te}_3\text{O}_9$ [26].

4. Conclusions

The family of ternary iron tellurate compounds shows a structural diversity that is characteristic for the stereochemistry of Fe^{2+} , Fe^{3+} , Te^{4+} , and Te^{6+} cations. Changing the Fe_3O_4 to TeO_2 ratio has the effect of creating structures with different valencies for the cations, or even mixed-valent structures. It should be possible, choosing the right proportions of iron and tellurium oxides, to synthesize *double*-mixed valent compounds, i.e. compounds containing both Fe^{2+} , Fe^{3+} , Te^{4+} , and Te^{6+} cations. The stereoactivity, and thus the structure dimension lowering effects of the Te^{4+} lone pairs becomes stronger if their concentration is higher. The overall tendency of the lone pairs is to push the Fe octahedra in two-dimensional (bi)layers. The lone pairs themselves are arranged in more or less regular tunnels.

References

- [1] O. Lindqvist, J. Moret, Acta Crystallogr. B 29 (1973) 643.
- [2] O. Lindqvist, W. Mark, J. Moret, Acta Crystallogr. B 31 (1975) 1255.
- [3] F. Daniel, J. Moret, M. Maurin, E. Philippot, Acta Crystallogr. B 34 (1978) 1782.
- [4] M. von Koçak, C. Platte, M. Trömel, Acta Crystallogr. B 35 (1979) 1439.
- [5] D. Hottentot, B.O. Loopstra, Acta Crystallogr. B 35 (1979) 728.
- [6] R. Astier, Ph.D. Thesis, Université des Sciences et Techniques du Languedoc, Montpellier, France, 1975.
- [7] J.-C. Jumas, M. Wintenberger, E. Philippot, Mater. Res. Bull. 12 (1977) 1063.
- [8] W. Kunmann, S.J. la Placa, L.M. Corliss, J.M. Hastings, E. Banks, J. Phys. Chem. Solids 29 (1968) 1359.
- [9] F. Pertlik, Tschermaks. Mineral. Petrogr. Mitt. 18 (1972) 39.
- [10] R. Astier, E. Philippot, J. Moret, J. Maurin, Rev. Chim. Miner. 13 (1976) 359.
- [11] G.C. Kennedy, Am. J. Sci. 248 (1950) 540.
- [12] CrysAlis RED, Oxford Diffraction Ltd., Version 1.171.31.5 (2006).
- [13] G. Oszlányi, A. Sütö, Acta Crystallogr. A 60 (2004) 134.
- [14] S. van Smaalen, L. Palatinus, M. Schneider, Acta Crystallogr. A 59 (2003) 459.
- [15] P.W. Betteridge, J.R. Carruthers, R.I. Cooper, K. Prout, D.J. Watkin, J. Appl. Crystallogr. 36 (2003) 1487.
- [16] M. Kroeker, L.W. Finger, Program DRAWxtl 5.1, (<http://www.lwfinger.net/drawxtl>), 2005.
- [17] A.S. Wills, I.D. Brown, VaList, CEA, France, 1999.
- [18] I.D. Brown, D. Altermatt, Acta Crystallogr. B 41 (1985) 244.
- [19] L. Glasser, H.D.B. Jenkins, J. Am. Chem. Soc. 122 (2000) 632.
- [20] J. Galy, G. Meunier, S. Anderson, A. Aström, J. Solid State Chem. 13 (1975) 142.
- [21] J.-M. Savariault, private communication; Crysat program, CEMES, Toulouse, France, 2006.
- [22] M. Kroeker, private communication, 2006.
- [23] A. Oufkir, M. Dutreilh, P. Thomas, J.-C. Champarnaud-Mesjard, P. Marchet, B. Frit, Mater. Res. Bull. 36 (2001) 693.
- [24] N. Barrier, S. Malo, O. Hernandez, M. Hervieu, B. Raveau, J. Solid State Chem. 179 (2006) 3484.
- [25] A. Chagraoui, A. Tairi, J.-C. Champarnaud-Mesjard, J. Phys. Chem. Solids 67 (2006) 2241.
- [26] E. Phillipot, R. Astier, W. Loeksmanto, M. Maurin, J. Moret, Rev. Chim. Miner. 15 (1978) 283.